DOI: 10.26599/FSHW.2026.9251055

Contents lists available at SciOpen

Food Science and Human Wellness

journal homepage: https://www.sciopen.com/journal/2097-0765

China Food Publishing Co.

A Rational Design and Development of a Label-free Fluorescent Biosensor for the Simultaneous and Rapid Detection of Five Fluoroquinolones in Food

Pingkang Xu [a], Guosheng Wang [a], Chi Xu [a], Yaning Song [a], Jie Tang [a,b], Xianggui Chen [a,b], Yukun Huang [a,b,d*], Dejian Huang [c,d]

[a] *School of Food and Biological Engineering, Food Microbiology Key Laboratory of Sichuan Province, Xihua University, Chengdu 610039, China*

[b] *Chongqing Key Laboratory of Speciality Food Co-Built by Sichuan and Chongqing, Chengdu 610039, China*

[c] *National University of Singapore (Suzhou) Research Institute, 377 Lin Quan Street, Suzhou Industrial Park, Suzhou, Jiangsu, 215123, China*

[d] *Department of Food Science and Technology, 2 Science Drive 2, National University of Singapore, 117542, Singapore*

ABSTRACT: Fluoroquinolones (FQs) are veterinary drug residues in the food chain that threaten global food safety and human health and there is a great need for a rapid, sensitive and reliable monitoring method to better safeguard our food systems. In this study, we developed a high-performance aptamer via a recognition-mechanism-oriented truncation strategy, enabling rapid and sensitive detection of multiple FQs. The recognition mechanism between the aptamer and FQs were studied by the combination of computer-aided molecular simulation and experimental verifications. It was revealed that hydrophobicity of FQs critically governs aptamer-target interactions. Guided by these insights, the original sequence was truncated to a 40-nt aptamer, named as W-G1, which preserved key binding sites and structural stability. W-G1 with the characteristic G-quadruplex (G4) conformation demonstrated excellent affinity and stability for FQs. Exploiting the function of this conformation, a label-free fluorescent G4/thioflavine T biosensor was fabricated to detect FQs in chicken ham sausage within 30 minutes. The results showed that detection limits ranged from 1.32 ng/kg to 17.30 ng/kg that are lower than food safety regulation defined limits of 1.0 μg/kg (the lowest LOD of standard method for lomefloxacin), with recoveries of 81.17~115.94%. This mechanism-driven strategy enhances aptamer-based detection of FQs, offering improved performance, design flexibility, and reduced cost.

Keywords: Fluoroquinolone; aptamer; recognition mechanism; rational design; detection

1. Introduction

Fluoroquinolones (FQs) are broad-spectrum antibiotics widely used to treat bacterial infections in humans and animals [1], representing the third largest class of antibiotics with 17% of the global market share (USD 7.1 billion) [2]. However, their extensive application in livestock and aquaculture has led to FQ residues in food and the environment, posing potential health risks [3]. Regulatory authorities have therefore imposed strict controls: the U.S. FDA banned enrofloxacin (ENR) in poultry in 2005, and China prohibited four FQs (lomefloxacin (LOW), pefloxacin (PEF), ofloxacin (OFL), and norfloxacin (NOR)) in food animals in 2015.

***Corresponding author**
hyk_diana@163.com

Received 9 September 2025
Received in revised from 20 October 2025
Accepted 2 December 2025

In addition, maximum residue limits (MRLs) for FQs have been established by the USA, European Commission, and China, generally requiring that FQs not be detectable in poultry and eggs, with MRLs for other foods ranging from 30 to 100 μg/kg.

Currently, high-performance liquid chromatography (HPLC) and liquid chromatography-mass spectrometry (LC-MS) are commonly employed for FQs determination. Nevertheless, trace-level residues and non-specific adsorption phenomena still pose considerable analytical challenges. The complex food matrices often interfere significantly with traditional chromatographic analyses, resulting in signal suppression and inaccurate quantification [4, 5]. Moreover, these conventional methods require costly instrumentation and experienced operators, restricting their accessibility for on-site or large-scale monitoring. To address these limitations, various biosensing approaches have attracted increasing attention owing to their high specificity, easy synthesis, and potential for low-cost, rapid detection [6].

Aptamers are short (15-100 nt) single-stranded oligonucleotides (ssDNA or RNA) with distinctive three-dimensional structures that can form stable complexes with target molecules. These structures are typically obtained via the systematic evolution of ligands by exponential enrichment (SELEX). Recently, researchers have identified several fluoroquinolone aptamers [7-10], among which Q8 is the most frequently used for FQ residue detection. Although these aptamers recognize similar FQ molecules, they differ markedly in both affinity and sequence composition. Previous studies have shown that certain nucleotides within aptamer sequences are nonessential for target recognition and may even destabilize the binding conformation [11, 12]. It is well established that oligonucleotides can fold into specific biological conformations with binding pockets that can be tailored for binding target molecules [13]. The reported original FQ aptamers average 76 nt in length (Table S1) and tend to form complex tertiary structures that hinder efficient sequence modification, reduce structural stability, and complicate practical analytical application. Therefore, for analytical applications, further optimization of the aptamer sequence is necessary to improve efficacy.

Conventional biosensing relies on fluorescent or radio labels to detect bio-molecular binding, but the labeling step increases time and cost, risks false negatives by occluding binding sites, introduces structural and functional interference, lacks specificity, and complicates conjugation [14, 15]. However, in the label-free detection, the signal is generated directly by the interaction between the analyte and the transducer. A label-free mode significantly reduces costs and minimizes the required expertise and effort to develop assays essentially by removing experimental artifacts such as quenching, and background fluorescence [16]. Beyond its conventional use in detecting amyloid fibrils, the water-soluble fluorescent probe thioflavin T (ThT) has also been reported to bind nucleic acids, inducing G-quadruplex (G4) formation and acting as a fluorescent sensor through enhanced emission. Notably, due to its high specificity for aptamers possessing these special structures, ThT is a promising candidate for use in label-free biosensors [17, 18].

Currently, computational simulation methods, such as molecular docking, are widely used for aptamer-target binding prediction and rationale design of selective aptamers [19, 20]. However, experimental techniques commonly used to validate these models and quantify binding include surface plasmon resonance

(SPR), isothermal titration calorimetry (ITC), biolayer interferometry (BLI) and microscale thermophoresis (MST) for kinetic/thermodynamic parameters, as well as circular dichroism (CD), fluorescence assays, and thermofluorimetric analysis (TFA) to monitor folding and conformational changes [21]. Therefore, to overcome these challenges, this study introduces a recognition-oriented truncation strategy that combines molecular recognition mechanism analysis with rational aptamer sequence optimization. Unlike previously reported empirical or random truncation methods, this approach is guided by structure–function insights to identify recognition-dominant domains and design shorter, high-performance aptamers with improved stability and affinity. Serving both as a recognition element and an efficient fluorescent probe, the proposed truncated aptamer-ThT complex was successfully employed to develop a label-free and homogeneous fluorescent biosensor for detecting multiple FQs in food. This mechanistically driven strategy not only elucidates the molecular recognition mechanism of broad-specificity FQ aptamers but also provides a novel, theoretically grounded framework for constructing aptamer-based sensing platforms with enhanced analytical performance for FQs residue monitoring

2. Material and methods

2.1 Materials

The single-stranded DNA oligonucleotides were synthesized by *Sangon Biotech Co., Ltd.* (Shanghai, China). Enrofloxacin (ENR), ciprofloxacin (CIP), ofloxacin (OFL), pefloxacin (PEF), lomefloxacin hydrochloride (LOW) amantadine, metronidazole, and furacilin were purchased from *Shanghai Yuanye Bio-Technology Co., Ltd*. (Shanghai, China). ThT was purchased from *Sigma Aldrich Trading Co., Ltd*. (Shanghai, China). Ultrapure water was provided by a Millipore Direct-Q UV purification apparatus (Bedford, MA, USA).

2.2 Methods

2.2.1 Secondary structure prediction and molecular docking

The chemical structures of FQs were shown in Figure S1. The predicted secondary structures of all the aptamers were obtained by *Mfold* program (http://unafold.rna.albany.edu/?q=mfold), *RNA Composer* (http://rnacomposer.ibch.poznan.pl/Home) was used as a freely available tool over the web for entirely automated prediction of the aptamer 3D structures. The 3D structure of FQs was obtained from the *PDB database*. A molecular docking study was performed to predict the binding mechanism between FQs and aptamers using the *AutoDock 4.2* program.

2.2.2 Experimental assays of recognition performance aptamer sequence

Dynamics and thermodynamics experiments were conducted by using MST, fluorescence spectroscopy [22] and ITC [23] to illustrate the mechanism of recognition interaction, respectively. Moreover, CD is utilized to investigate the conformational polymorphism of nucleic acids and FQs [24]. The detailed information of the relative methods and instruments employed is introduced in *Supporting information*.

2.2.3 Design and assessment of truncated aptamer

The binding sites of five FQs were obtained from molecular docking and 2-aminopurine (2-AP) fluorescence analyses (see *Supporting Information* and Table S2) [25]. Two truncation methods were developed based on the key binding sites and binding regions suggested from the mechanistic study. The first truncation approach targeted key sites and applied region-specific trimming to the aptamer and its targets (CIP, ENR, OFL, PEF, and LOW), whereas the second approach sought to preserve the W aptamer's stem-loop truncation pattern. Approach I refers to the truncation strategy applied to the W-G series, including W-G1 and W-G2. Approach II, on the other hand, represents the design of the W-J series, which was developed based on the W-G structural framework. Finally, affinity and selectivity assays were conducted to evaluate the performance of the truncated aptamers (details in *Supporting Information*) [26].

2.2.4 Optimization of label-free G4/ThT fluorescent aptasensor based on truncated aptamer

2.2.4.1 Truncated aptamer/ThT ratio

The truncated aptamer (designated W-G1) was prepared at a fixed concentration of 200 nmol/L and then serially diluted at ratios of 1:10, 1:20, 1:50, 1:100, and 1:150. Each W-G1 dilution was mixed with ThT at a 1:1 volume ratio and incubated at 25 °C for 30 min. After incubation, samples were transferred to a 1 mm-pathlength quartz cuvette, and fluorescence spectra were recorded on a FluoroMax-4P spectrometer (λ_{ex} = 425 nm; λ_{em} = 450~600 nm; slit width = 5 nm; data interval = 1 nm).

2.2.4.2 Incubation time of ThT

Using the optimal W-G1/ThT ratio, W-G1 and ThT were mixed, and fluorescence spectra were recorded at 0 min, 5 min, 10 min, 15 min, 20 min, 25 min, and 30 min. Each FQ solution (300 nmol/L) was prepared and incubated in 5-minute increments up to 30 min; after each interval, fluorescence intensity was measured. Subsequently, an equivalent aliquot of fresh FQ was added, and the mixture was re-incubated under the same time course, with fluorescence intensity measured again.

2.2.5 Detection of five FQs in food based on label-free fluorescent aptasensor

2.2.5.1 Preparation of food sample for detection

Chicken ham sausages were purchased from *Walmart* Supermarket in Pidu District, Chengdu. Twenty-five grams of ham sausage were homogenized and then spiked with a standard FQs solution. Two grams of the spiked homogenate were extracted by ultrasonication in 5 mL of acetonitrile for 5 min. After centrifugation at 10 000 rpm for 5 min, the supernatant was filtered through a 0.45 μm membrane, evaporated to dryness under a gentle nitrogen stream, and reconstituted in 5 mL of binding buffer. This procedure yielded spiked test solutions at 18.00 μg/kg, 54.00 μg/kg, and 90.00 μg/kg.

2.2.5.2 Establishment of label-free fluorescent aptasensor for FQs detection

Under the optimal conditions described above, W-G1 and ThT were combined in a tube and incubated in the dark at 25 °C for 5 min, then the initial fluorescence intensity (F_0) was recorded. Equal volumes of varying concentrations of FQs (ENR, CIP, LOW, PEF, and OFL) were then added, and the mixture was incubated in

the dark at 25 °C for an additional 15 min before measuring the stable fluorescence intensity (F_1). A calibration curve was constructed by plotting lgC_{FQs} on the x-axis against ΔF (F_0-F_1) on the y-axis.

3. Results and discussion

3.1 Revelation of mechanism of the broad-selectivity aptamer recognizing FQs molecules

3.1.1 Molecular docking of binding between FQs and aptamers

This work builds on prior studies, most of which identified and validated aptamers for FQ recognition [8-10]. Computer-aided molecular docking significantly expands the possibilities for aptamer design and optimization [27]. The five FQs investigated in this study possess both hydrophobic groups (such as aromatic rings and carbonyl groups) and hydrophilic groups (carboxyl groups), with varying degrees of hydrophobicity (hydrophobicity order: OFL < CIP < PEF < LOW < ENR). As shown in Figure 1, upon docking with the aptamer, the binding free energies between the FQs and the aptamers—calculated using *Auto Dock Tools 1.5.6*—were all below -6.9 kcal/mol (Table S3), indicating the formation of thermodynamically stable complexes and a strong affinity between the aptamers and FQs. The interaction between the target molecules and aptamers is primarily driven by structural complementarity and non-covalent forces, including hydrogen bonding, T-shaped π–π interactions, and hydrophobic interactions [2]. The molecular docking analysis revealed specific interaction patterns between aptamers and FQs. Notably, both the hydrophobic groups (aromatic rings and carbonyl groups) and the hydrophilic carboxyl groups of FQs were inferred to play crucial roles in binding. The aromatic rings and carbonyl groups were involved in forming hydrophobic interactions, including T-shaped stacking, with the nucleotide bases of the aptamer. In contrast, the carboxyl groups formed hydrogen bonds with aptamer bases. Additionally, the -R3 substituents (e.g., methyl or cyclopropyl groups) in FQs, due to their structural flexibility, tended to interact with aptamer bases via hydrophobic interactions. The combination of these forces collectively mediates the aptamer-FQ binding and contributes to the formation of stable aptamer–antibiotic complexes. To sum up, the hydrophobic and hydrophilic groups and fluorine atom of FQs play a significant role in FQs binding to aptamers.

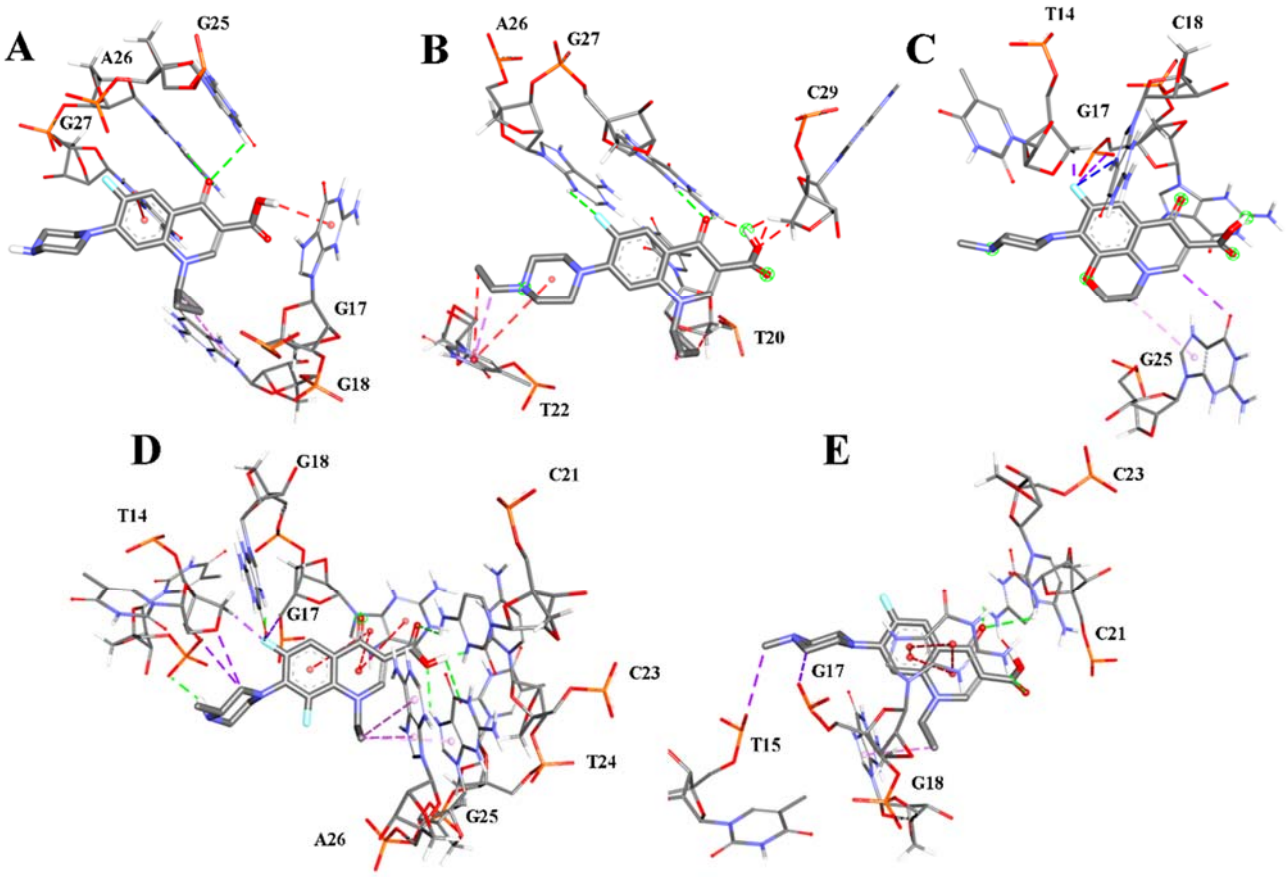

Figure 1. Docking models of aptamer W with targets: (A)CIP; (B)ENR; (C)OFL; (D)LOW; (E)PEF (Conventional hydrogen bond interaction is presented as green dotted lines, pink dotted lines indicate Pi-Alkyl interaction, red dotted lines indicate Pi-Pi stacked interaction, blue dotted lines indicate Halogen (Fluorine) interaction, and purple dotted lines indicate carbon hydrogen bond interaction)

3.1.2 Laboratory testing of binding between FQs and aptamers

After the theoretical model, furthermore, laboratory testing is essential to demonstrate that the aptamer functions effectively as a recognition element through its binding interactions. The subsequent analyses were performed to elucidate the recognition mechanism by using MST, fluorescence spectroscopy, and ITC, respectively. MST was employed to validate the binding affinities between the aptamers and FQs (Figure S2 and Table S4). Additionally, CD spectroscopy was employed to assess the conformational polymorphism of nucleic acids and FQs, providing insights into the structural characteristics of aptamer-FQ complexes [28-30]. It was found that FQs can induce Q-series aptamers to transition from B-DNA to A-DNA [11, 31, 32] or C-DNA [33], and can either promote W aptamers to adopt a more stable G4 structure [34] or destabilize the existing G4 structure (Figure S3) [35]. These findings are consistent with the MST and molecular-docking data, confirming a hydrophobic interaction between W and the five FQs. The CD spectra (Figure S3) and ITC (Figure S4) results further support this interaction, highlighting its significance in elucidating the aptamer-target binding mechanism and informing aptamer sequence optimization.

3.1.3 Confirmation of the binding site between FQs and aptamers

Moreover, 2-AP assay is widely employed to monitor DNA conformational dynamics, as it forms a canonical Watson-Crick base pair with thymine while exerting minimal perturbation on native structure. By

substituting for adenine in oligonucleotides, 2-AP serves as an effective intrinsic fluorophore. In this study, we exploit the fluorescence intensity change of a 2-AP–labeled aptamer upon target binding to pinpoint critical nucleobase positions. Therefore, ley nucleotides responsible for FQ recognition were identified through a combination of molecular docking (Table S4) and 2-AP fluorescence (Figure 2) assays, laying the theoretical groundwork for subsequent truncation optimization. The most pronounced fluorescence changes upon FQs binding were observed at W-A20, W-A21, and W-A49 (Figure 2c), respectively, indicating that these sites are critical for the W aptamer's interaction with FQs. This insight is essential for refining truncation strategies to develop aptamers with improved affinity and selectivity.

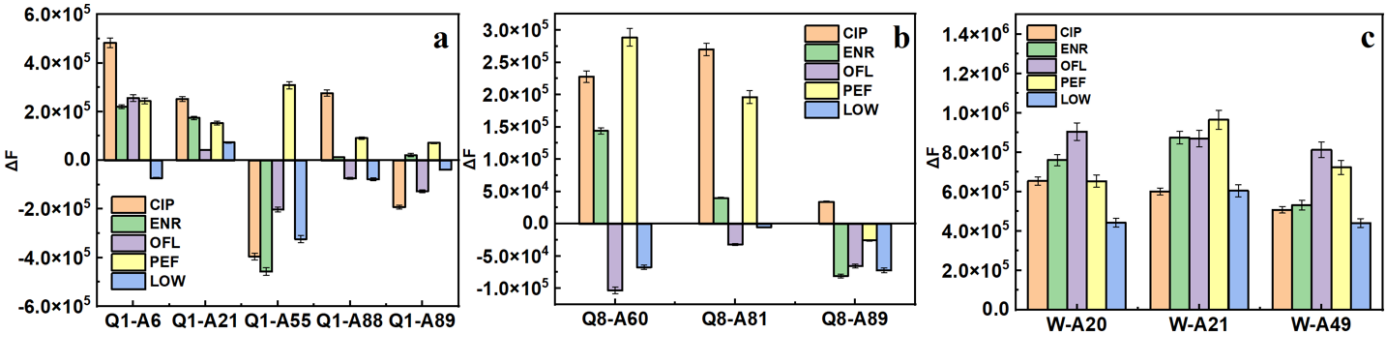

Figure 2. Difference of fluorescence intensity between aptamers (bases were replaced by 2-AP) and target before and after binding. F_0-F>0 indicates fluorescence enhancement, F_0-F<0 indicates fluorescence quenching.) (a) 2-AP substitutes bases Q1-A6, A21, A55, A88 obtained sequences Q1-A6, Q1-A21, Q1-A55, Q1-A88, Q1-A89. (b) 2-AP substitutes base of Q8 to get sequences Q8-A60, Q8-A81, Q8-A89; (c) 2-AP replaces bases of W to get sequences W-A20, W-A21, W-A49, W-A89

3.2 Truncation design and confirmation analysis of aptamer W-G1

3.2.1 Conception of truncation design of aptamers

To eliminate systematic errors arising from methodological differences, the affinities of seven aptamers for five fluoroquinolones were assessed using a unified standard—combining molecular docking with experimental assays. The results revealed that three aptamers (Q1, Q8, and W) exhibited high affinity toward all five compounds. However, previous studies have shown that truncation of Q1 or Q8 markedly diminishes their binding strength [8]. Accordingly, aptamer W was selected for the subsequent truncation design.

In general, the G4 structure enhances the aptamer's thermal and chemical stability during target recognition [36, 37]. Given its characteristic G4 motif and high affinity for all five fluoroquinolones, aptamer W was chosen as the candidate for truncation optimization. Based on the elucidated binding conformation, five truncated variants (W-G1, W-G2, W-J1, W-J2, and W-J3) were then designed (Table 1). Their predicted secondary structures were modeled using the *Mfold* web server. As shown in Figure 3, all truncated aptamers preserved the characteristic stem-loop structure of aptamer W, indicating that excision of redundant bases did not compromise the overall aptamer conformation in theory.

Table 1. Rational design of truncation aptamer sequences of FQs

Name	Sequence (5'-3')
W-G1	TAG GCT AAC ACG GTT CGG CTC TCT GAG CCC GGG TTA TTT C
W-G2	AAC ACG GTT CGG CTC TCT GAG CCC GGG TT
W-J1	CGG TTC GGC TCT CTG AGC CCG
W-J2	CTC TCT GAG
W-J3	CGG TTC GGC CCG

Name	Sequence (5'-3')
W	CCC ATC AGG GGG CTA GGC TAA CAC GGT TCG GCT CTC TGA GCC CGG GTT ATT TCA GGG GGA

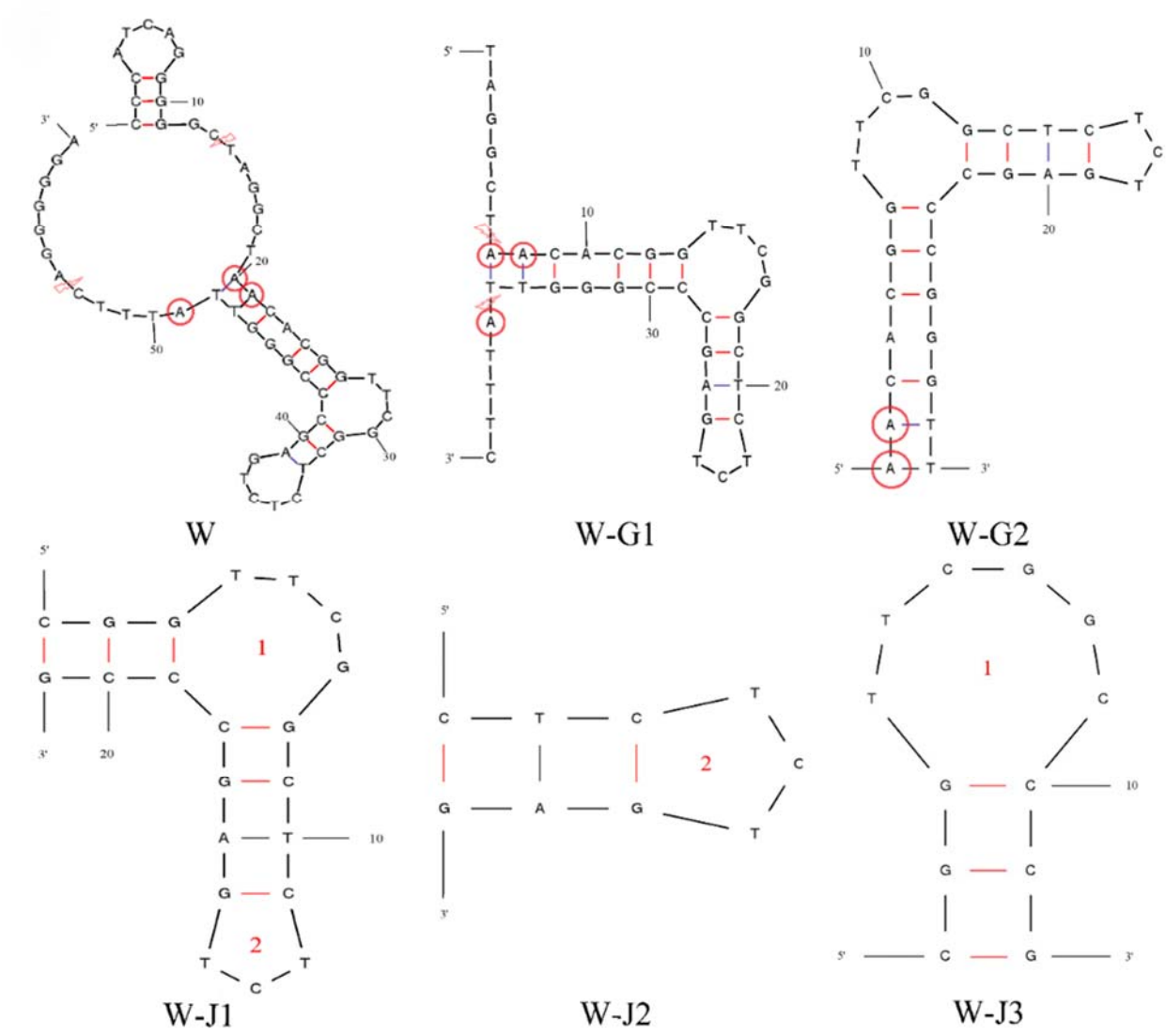

Figure 3. Rational design of W aptamer truncation

3.2.2 Characterization of affinity between truncated aptamers and FQs

As presented in Table S5 and Figure 4, the truncated aptamers demonstrated varying degrees of enhanced affinity for the fluoroquinolones. A comparative summary of their affinities and binding sites is shown below:

(1) W-G1 retained the original W aptamer's key binding sites (A20, A21, and A49) and exhibited dramatically enhanced affinities by178-fold for ENR, 41-fold for OFL, and 72-fold for LOW, respectively. Although the other truncated variants showed some affinity improvements, none reached such high levels. Therefore, W-G1 demonstrated the highest binding strengths for ENR, OFL, and LOW, making it the most effective candidate.

(2) W-J1 displayed the greatest affinity for CIP, with an 89.3-fold increase. Deletion of the original key sites (A20, A21, and A49) in W-J1 induced a conformational shift, enabling recognition via a novel binding site. Notably, W-J1 preserved both stem-loop structures of the parent W aptamer, whereas W-J2 and W-J3

each retained only one. The comparatively lower CIP affinity of W-J2 and W-J3 indicates that the dual stem-loop configuration in W-J1 is optimal for effective CIP binding.

(3) W-J2 exhibited the greatest affinity for PEF, with a 67-fold enhancement, underscoring the critical role of the stem-loop motif in PEF recognition. However, although both W-J2 and W-J3 outperformed the parent W aptamer in affinity, their structural stability was markedly compromised.

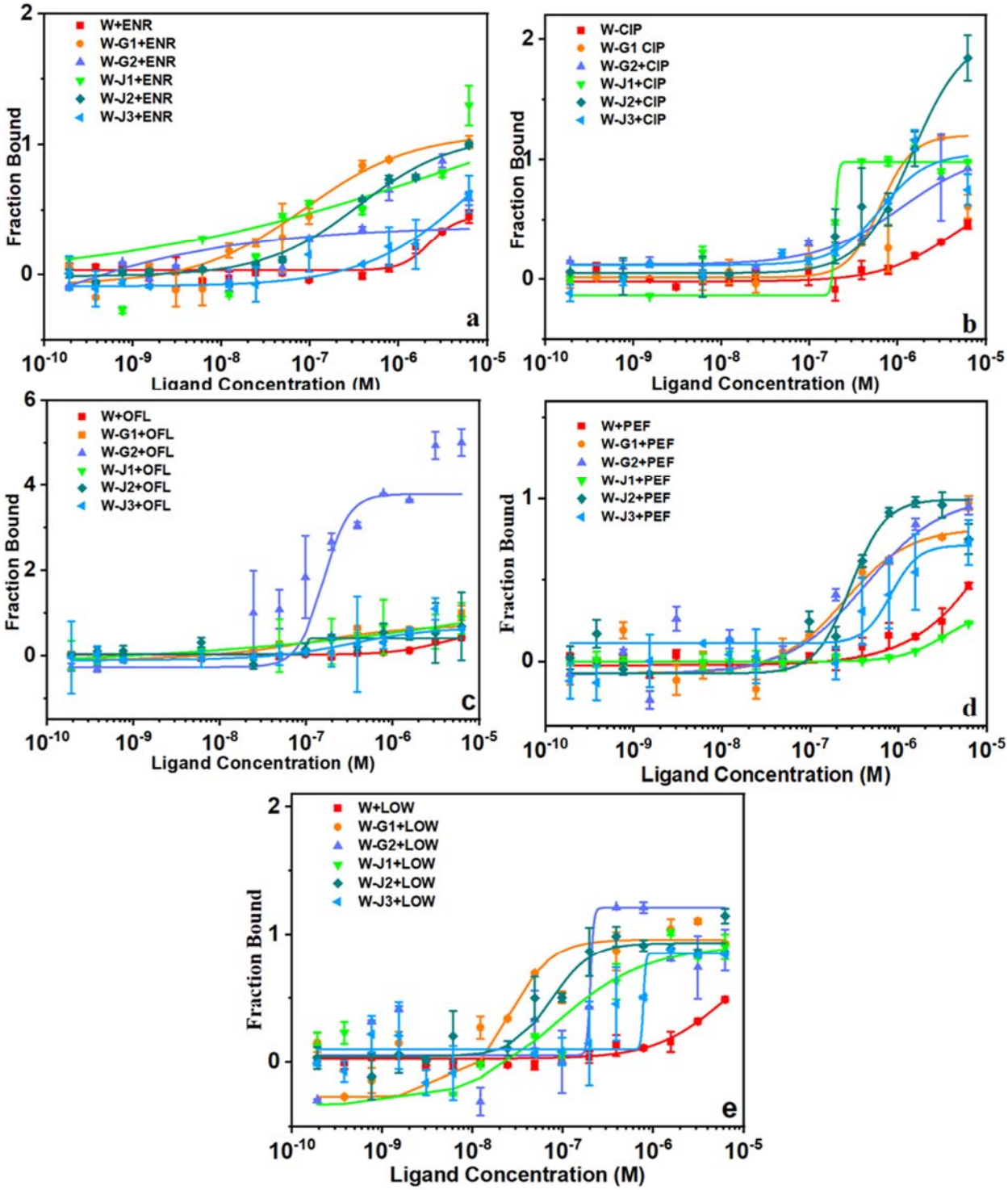

Figure 4. The affinity between aptamer and FQs was characterized by MST. (a) ENR, (b) CIP, (c) OFL, (d) PEF, (e) LOW.

The loss of a stem-loop in W-J1, W-J2, and W-J3 resulted in diminished stability and weakened FQ interactions, which further underscore the necessity of the dual stem-loop architecture for effective

recognition of all five FQs. In contrast, W-G1 combined exceptional affinity with robust structural integrity across all five target FQs, establishing it as the premier candidate. Consequently, W-J1, W-J2, and W-J3 were excluded from further studies.

3.2.3 Selectivity of new W-G1

As shown in Figure 5, W-G1 exhibited excellent selectivity for the five FQs, with minimal response to non-target substances such as amantadine, metronidazole, and furacilin—common veterinary drug residues in animal-derived food. Consequently, W-G1 was identified as the short-chain aptamer with outstanding affinity and selectivity among all candidates evaluated.

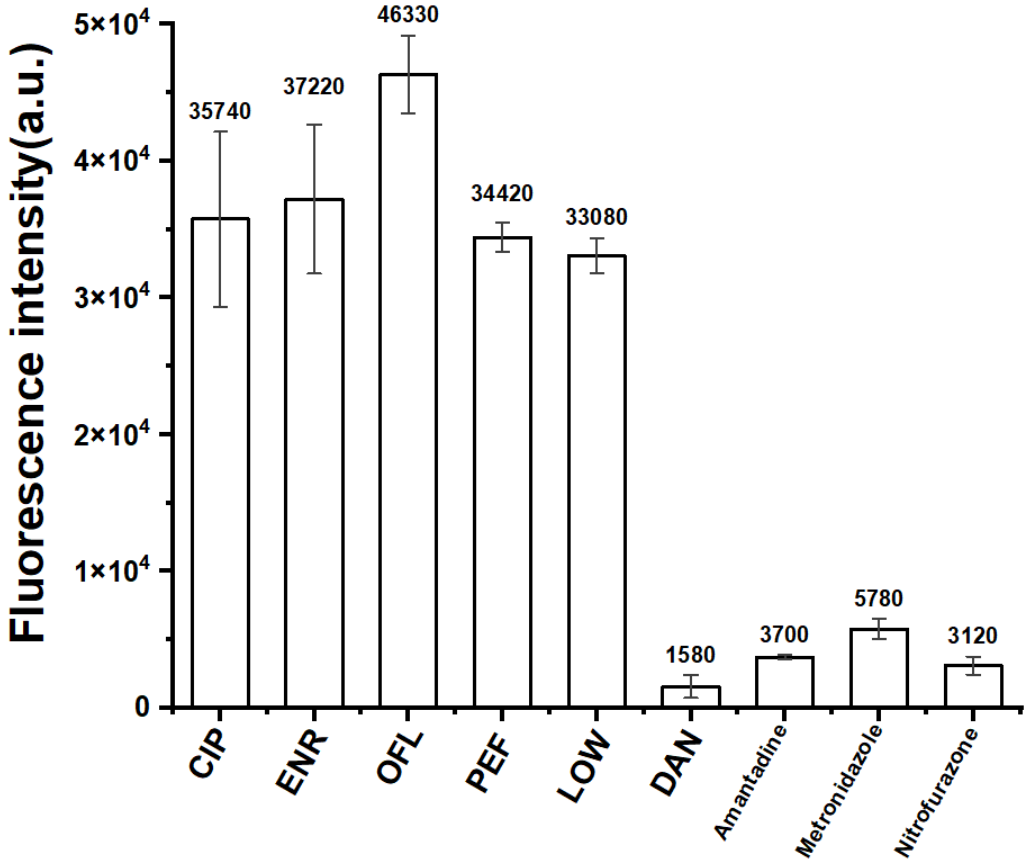

Figure 5. Specific selection of W-G1 for FQs.

3.3 Detection of FQs using W-G1 in a G4/ThT-based fluorescent aptasensor

3.3.1 Principle of the label-free fluorescent aptasensor

The working principle of the label-free G4/ThT fluorescent aptasensor is illustrated in Figure 6. In the absence of FQs, W-G1 adopts a conformation that readily folds into a G4, allowing free ThT to intercalate and generate a strong fluorescence signal. Upon introduction of FQs, W-G1 preferentially binds to the targets, instigating a competition of FQs molecules and ThT and resulting in a corresponding decrease in fluorescence intensity.

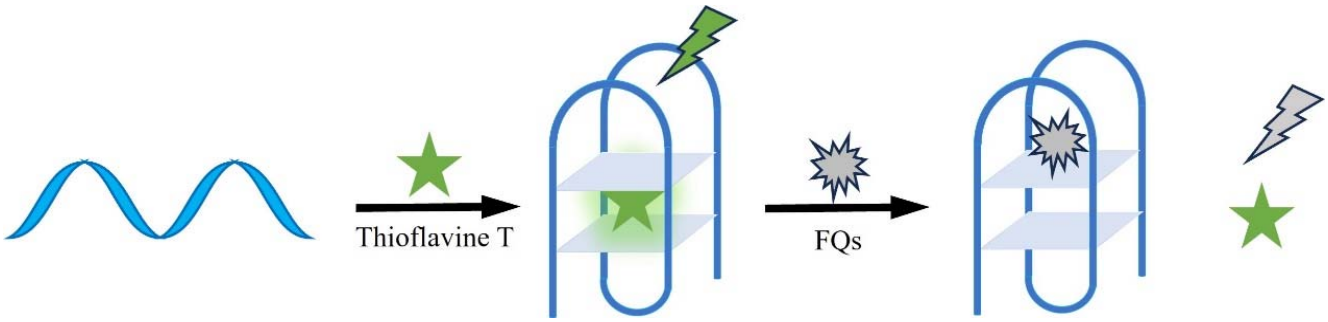

Figure 6. Schematic description of a label-free fluoresecent aptasensor for FQs detection based on G4/ThT

3.3.2 The optimization assay of detection

To improve the analytical performance of the assay for FQs, the key parameters affecting sensitivity and selectivity were optimized: the W-G1/ThT ratio, ThT incubation time, and FQs incubation time.

As shown in Figure 7a, the fluorescence intensity rose markedly as the W-G1/ThT ratio increased from 1:10 to 1:150, while declined sharply at 1:200. Consequently, the optimal ratio was determined to be 1:150, corresponding to 200 nmol/L W-G1 and 30 μmol/L ThT.

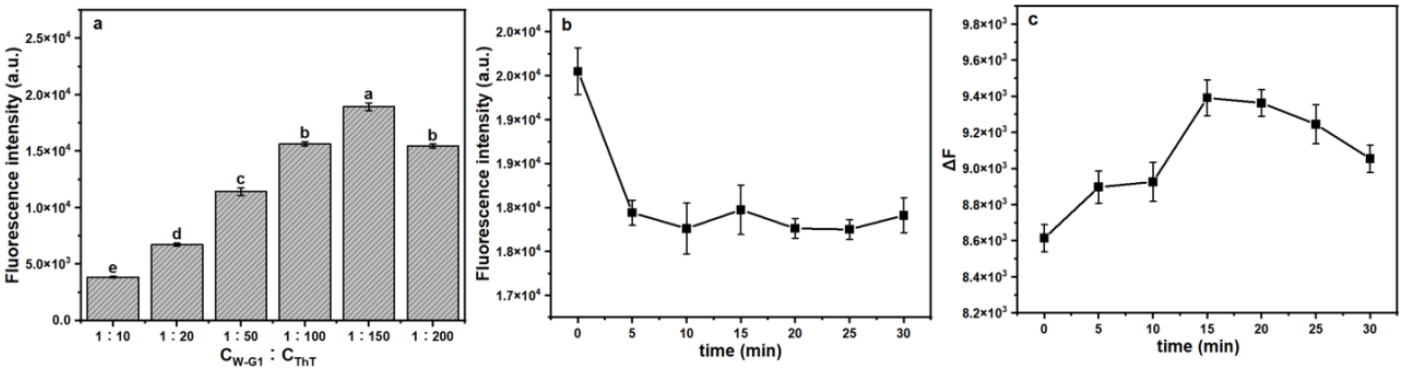

Figure 7. Results of optimized conditions for detection. (a)W-G1/ThT ratio optimization, (b) ThT incubation time optimization, (c) FQs incubation time optimization.

ThT exhibited rapid fluorescence decay under various conditions. To determine the optimal measurement time, we examined the relationship between ThT fluorescence intensity and incubation time. As shown in Figure 7b, the signal declined obviously during the first 0~5 min before stabilizing. Accordingly, to maximize detection accuracy, the W-G1/ThT incubation time was set to 5 min.

Incubation time between the target and aptamer can significantly affect their binding and, consequently, the ThT fluorescence signal. To optimize this parameter, we measured ThT fluorescence after incubating FQs with W-G1 for varying durations. As illustrated in Figure 7c, fluorescence intensity increased with longer incubation times, reaching a maximum at 15 min. Therefore, 15 min was selected as the optimal incubation time for FQs.

3.3.3 Analytical performance of the method

To assess W-G1's potential for detecting multiple FQs, we generated standard curves for all five compounds using the label-free G4/ThT fluorescent aptasensor. As shown in Table 2, the calibration equations and limits of detection (LODs) for each FQ exhibited broad linear ranges covered nearly two orders of magnitude and low LODs ranged from 1.32±0.09 ng/kg to 17.30±0.10 ng/kg.

Table 2. Analytical performance of detection for five FQs

FQs	Standard curve	R	Linear range	LOD (ng/kg)
ENR	$\Delta F=382.75\lg C_{ENR}+8902.69$	0.9975	8.98 ng/kg~89.85 μg/kg	1.92±0.08
LOW	$\Delta F=571.44\lg C_{LOW}+10686.45$	0.9990	9.70 ng/kg~0.97 μg/kg	2.19±0.12
CIP	$\Delta F=175.45\lg C_{CIP}+10036.21$	0.9955	82.84 ng/kg~0.83 μg/kg	1.32±0.09
PEF	$\Delta F=164.74\lg C_{PEF}+9384.39$	0.9925	9.79 ng/kg~116.37 μg/kg	17.30±0.10
OFL	$\Delta F=272.47\lg C_{OFL}+8018.85$	0.9955	9.03 ng/kg~0.09 μg/kg	11.35±0.08

3.3.4 Application of the method in analysis of FQs in foods

Spike-recovery experiments were performed by adding five FQs at three concentration levels (18.00, 54.00, 90.00 μg/kg) into chicken ham sausage sample. As shown in Table 3, recoveries across the 15 sample groups ranged from 81.17% to 115.94%, demonstrating the high accuracy of W-G1 for FQ detection in food. The RSDs of assays were lower than 7%. These results highlight the promising potential of the W-G1 aptamer for simultaneous detection of multiple FQs in food matrices. Furthermore, compared to previously reported methods for the simultaneous detection of multiple FQs (Table 4), the developed approach significantly reduces the whole detection time by eliminating time-consuming steps such as fixation, labeling, and modification. In addition, it enables the detection of a lower LODs of targets, thereby fulfilling the requirements for monitoring banned FQs.

Table 3. Spiked recoveries in real samples

FQs	Backgrouds (μg/kg)	Spiked (μg/kg)	Found (μg/kg)	Recovery(%)	RSD(%)
	0.00	18.00	15.90±0.13	88.36	6.59
ENR	0.00	54.00	57.37±0.68	106.25	7.00
	0.00	90.00	81.45±2.05	90.49	5.24
	0.00	18.00	16.92±0.21	90.02	3.91
LOW	0.00	54.00	47.03±1.27	87.09	4.64
	0.00	90.00	95.44±3.03	106.04	5.60
	0.00	18.00	16.25±0.98	90.26	4.24
CIP	0.00	54.00	62.61±2.15	115.94	3.29
	0.00	90.00	83.45±4.62	92.72	6.08
	0.00	18.00	12.58±0.93	83.71	4.10
PEF	0.00	54.00	56.11±2.07	103.56	6.76
	0.00	90.00	108.12±6.55	114.68	6.73
	0.00	18.00	20.34±0.73	112.99	5.31
OFL	0.00	54.00	43.83±1.94	81.17	5.24
	0.00	90.00	98.21±5.81	109.12	6.60

Table 4. Comparison with other reported methods for the simultaneous detection of FQs

Method	Analytes	Principle	Core elements	Detection time	Limit of detection	Reference
Terbium (III) and aptamer-based probe	Enrofloxacin, Norfloxacin, Ciprofloxacin	Molecular recognition	Aptamer (60-nt, NH_2-3' labeled), $TbCl_3$ solution	Incubation time of 30 min	Enrofloxacin: 61 ng/L Norfloxacin: 20 ng/L Ciprofloxacin: 53 ng/L	[38]
Lateral flow immune-chromatography	Enrofloxacin, Ciprofloxacin, Flumequine, Marbofloxacin, Oxolinic acid, Danofloxacin	Immuno-chromatography	Four antibodies, gold nanoparticule, anti-mouse IgG, BSA, nitrocellulose membrane	Assay time ranging between 4 and 8 min	Enrofloxacin: 50 μg/kg Ciprofloxacin: 50 μg/kg Flumequine: 100 μg/kg Marbofloxacin: 75 μg/kg Oxolinic acid: 50 μg/kg Danofloxacin: 50 μg/kg	[39]

Triple-channel sensor array	Enrofloxacin, Ofloxacin, Pefloxacin, Norfloxacin, Ciprofloxacin, Enrofloxacin, Gatifloxacin, Sparfloxacin	Fingerprint recognition	Nitrogen-sulfur co-doped carbon dots, Cu^{2+}, Fe^{3+}, PCA or HCA	Incubation time of 10 min	Enrofloxacin: 216.0 μg/L Ofloxacin: 83.1 μg/L Pefloxacin: 215.6 μg/L Norfloxacin: 115.0 μg/L Ciprofloxacin: 70.6 μg/L Enrofloxacin: 81.0 μg/L Gatifloxacin: 378.7 μg/L Sparfloxacin: 286.1 μg/L	[40]
Label-free fluorescent aptasensor	Enrofloxacin, Lomefloxacin, Ciprofloxacin, Pefloxacin, Ofloxacin	Molecular recognition	Aptamer (40-nt, label-free), ThT	Whole detection time is less than 30 min, including sample preparation and incubation time	Enrofloxacin: 1.92 ng/kg Lomefloxacin: 2.19 ng/kg Ciprofloxacin: 1.32 ng/kg Pefloxacin: 17.30 ng/kg Ofloxacin: 11.35 ng/kg	This work

4. Conclusion

In summary, a creative 40-nt FQs aptamer W-G1 was gained, which proved to be superior to the original 60-nt W aptamer in recognition performance after systematic comparisons. Moreover, the detection limits of the established aptasensor were 1.32~17.30 ng/kg, with recovery rates ranged from 81.17% to 115.94%. This study establishes a practical approach to elucidate the theoretical basis of aptamer-target recognition and to develop a rational truncation strategy. It thus lays the groundwork for the application of short-chain FQ aptamers with enhanced performance in food analysis.

Supporting Information

The Supporting Information is available free of charge at ***

A comprehensive description of the experimental procedures, accompanied by the corresponding results and a discussion elucidating and validating the conformational recognition mechanism between FQs and their aptamers, including representative microscale thermophoresis binding curves, CD spectra, ITC profiles for the binding of FQs to aptamers, specific experiment. (PDF)

Funding Sources

This research was funded by the National Natural Science Foundation of China (31801647), Science and Technology Project of Administration for Market Regulation Sichuan Province (SCSJS2025014). This paper has received the supporting from China Scholarship Council.

Notes

The authors declare no competing financial interest.

References

[1] Huang, Y. K.; Wang, C.; Wei, Q. M.; Song, Y. N.; Chen, P. F.; Wang, L. J.; Yang, X.; Chen, X. G. A sensitive aptasensor based on rolling circle amplification and G-rich ssDNA/terbium (III) luminescence enhancement for ofloxacin detection in food. *Talanta* **2021**, *235*.

[2] Zou, M. Y.; Tian, W. J.; Zhao, J.; Chu, M. L.; Song, T. T. Quinolone antibiotics in sewage treatment plants with activated sludge treatment processes: A review on source, concentration and removal. *Process Saf Environ* **2022**, *160*, 116–129.

[3] Yan, G.H.; Zhang, S.H.; Han, Z., Yi, S.S.; Wang, Y.; Zhu, L.L.; Zhang, L.Y. Construction of a sensor array using TiO2 NRs/CuO/rMIP with imprinted sites regulation as light-activated nanozyme to colorimetric detect fluoroquinolones. *Sens. Actuators B Chem* **2024**, *419*, 136373.

[4] Liu, W. X.; Song, S.; Ye, M. L.; Zhu, Y.; Zhao, Y. G.; Lu, Y. Nanomaterials with Excellent Adsorption Characteristics for Sample Pretreatment: A Review. *Nanomaterials-Basel* **2022**, *12* (11), 1845.

[5] Liang, D., Xu, Y., Peng, F., Ma, W., & Zhao, Y. Plasmonic metal NP-bismuth composite film with amplified SERS activity for multiple detection of pesticides and veterinary drugs. *Chem. Eng. J.* **2023**, *474*, 145933.

[6] Ouyang, Y. C., Yeom, B. J., Zhao, Y., & Ma, W. Progress and prospects of chiral nanomaterials for biosensing platforms. *Rare Met.* **2024,** *43* (6), 2469-2497.

[7] Liu, X. H.; Wang, Z. C.; Zhang, X. B.; Xu, D. K. Screening of Lomefloxacin Aptamers Based on Polydopamine Nanospheres. *Chinese J Anal Chem* **2017**, *45* (12), 1971–1979.

[8] Reinemann, C.; von Fritsch, U. F.; Rudolph, S.; Strehlitz, B. Generation and characterization of quinolone-specific DNA aptamers suitable for water monitoring. *Biosens Bioelectron* **2016**, *77*, 1039–1047.

[9] Liu, X. Y.; Ren, J.; Su, L. H.; Gao, X.; Tang, Y. W.; Ma, T.; Zhu, L. J.; Li, J. R. Novel hybrid probe based on double recognition of aptamer-molecularly imprinted polymer grafted on upconversion nanoparticles for enrofloxacin sensing. *Biosens Bioelectron* **2017**, *87*, 203–208.

[10] Ni, H. J.; Zhang, S. X.; Ding, X. H.; Mi, T. J.; Wang, Z. H.; Liu, M. X. Determination of Enrofloxacin in Bovine Milk by a Novel Single-Stranded DNA Aptamer Chemiluminescent Enzyme Immunoassay. *Anal Lett* **2014**, *47* (17), 2844–2856.

[11] Jia, M.; Sha, J. Y.; Li, Z. H.; Wang, W. J.; Zhang, H. Y. High affinity truncated aptamers for ultra-sensitive colorimetric detection of bisphenol A with label-free aptasensor. *Food Chem* **2020**, *317*.

[12] Han, X.; Qin, M.W.; Lu, X.D.; Wang, Q.D.; Zhang, Y.; Wang, Z.P. A highly sensitive SERS aptasensor using a novel truncated aptamer for the detection of Deoxynivalenol. *Sens. Actuators B Chem* **2025**, *424*, 136908.

[13] Xiao, X. N.; Zhu, L. J.; He, W. C.; Luo, Y. B.; Xu, W. T. Functional nucleic acids tailoring and its application. *Trac-Trend Anal Chem* **2019**, *118*, 138–157.

[14] Kim, J.; Campbell, A. S.; de Avila, B. E. F.; Wang, J. Wearable biosensors for healthcare monitoring. *Nat Biotechnol* **2019**, *37* (4), 389–406.

[15] Vollmer, F.; Arnold, S. Whispering-gallery-mode biosensing: label-free detection down to single molecules. *Nat Methods* **2008**, *5* (7), 591–596.

[16] Zhang, Y.; Hu, Y.; Deng, S.; Yuan, Z.L.; Li, C.H.; Lu, Y.H; He, Q.; Zhou, M.; Deng, R.J. Engineering Multivalence Aptamer Probes for Amplified and Label-Free Detection of Antibiotics in Aquatic Products. *J. Agric. Food Chem.* **2020**, *68* (8), 2554-2561.

[17] Khusbu, F. Y.; Zhou, X.; Chen, H. C.; Ma, C. B.; Wang, K. M. Thioflavin T as a fluorescence probe for biosensing applications. *Trac-Trend Anal Chem* **2018**, *109*, 1–18.

[18] Zhao, L. L.; Gu, Y. X.; Dong, J. H.; Li, X. T.; Pan, H. Y.; Xue, C. Y.; Liu, Y.; Zhou, Y. L.; Zhang, X. X. New G-Triplex DNA Dramatically Activates the Fluorescence of Thioflavin T and Acts as a Turn-On Fluorescent Sensor for Uracil-DNA Glycosylase Activity Detection. *Anal Chem* **2024**, *96* (21), 8458–8466.

[19] Tao, X.; Huang, Y. K.; Wang, C.; Chen, F.; Yang, L. L.; Ling, L.; Che, Z. M.; Chen, X. G. Recent developments in molecular docking technology applied in food science: a review. *Int J Food Sci Tech* **2020**, *55* (1), 33–45.

[20] Buglak, A. A.; Samokhvalov, A. V.; Zherdev, A. V.; Dzantiev, B. B. Methods and Applications of In Silico Aptamer Design and Modeling. *Int J Mol Sci* **2020**, *21* (22).

[21] Brown, A., Brill, J., Amini, R., Nurmi, C., & Li, Y.F. Development of better aptamers: structured library approaches, selection methods, and chemical modifications. *Angew. Chem. Int. Ed.* **2024**, *63* (16), e202318665.

[22] Sohrabijam, Z.; Saeidifar, M.; Zamanian, A. Enhancement of magnetofection efficiency using chitosan coated superparamagnetic iron oxide nanoparticles and calf thymus DNA. *Colloid Surface B* **2017**, *152*, 169–175.

[23] Su, T. J.; Connolly, B. A.; Darlington, C.; Mallin, R.; Dryden, D. T. F. Unusual 2-aminopurine fluorescence from a complex of DNA and the EcoKI methyltransferase. *Nucleic Acids Res* **2004**, *32* (7), 2223–2230.

[24] Ponkarpagam, S.; Vennila, K. N.; Elango, K. P. Investigating binding of insecticide buprofezin to DNA by experimental and metadynamics simulation studies. *J Biomol Struct Dyn* **2023**, *41* (8), 3476–3484.

[25] Marky; L, A.; Breslauer; K, J. Origins of netropsin binding affinity and specificity: correlations of thermodynamic and structural data. *Proceedings of the National Academy of Sciences of the United States of America* **1987**.

[26] Huang, Y. K.; Chen, X. J.; Duan, N.; Wu, S. J.; Wang, Z. P.; Wei, X. L.; Wang, Y. F. Selection and characterization of DNA aptamers against enterotoxin C1. *Food Chem* **2015**, *166*, 623–629.

[27] Chen, P.F; Hu, C.Q.; Tao, X.; et al.. Recognition mechanism and sequence optimization of organophosphorus pesticides aptamers for better monitoring contaminations in food. *Food Science and Human Wellness* 2023, *12*(5): 1708-1715.

[28] Kypr, J.; Kejnovská, I.; Renciuk, D.; Vorlícková, M. Circular dichroism and conformational polymorphism of DNA. *Nucleic Acids Res* **2009**, *37* (6), 1713–1725.

[29] Chen, L. M.; Liu, J.; Chen, J. C.; Tan, C. P.; Shi, S.; Zheng, K. C.; Ji, L. N. Synthesis, characterization, DNA-binding and spectral properties of complexes [Ru (L) 4 (dppz)]$^{2+}$(L= Im and MeIm). *J Inorg Biochem* **2008**, *102* (2), 330–341.

[30] Kumar, M.; Kaushik, M.; Kukreti, S. Interaction of a photosensitizer methylene blue with various structural forms (cruciform, bulge duplex and hairpin) of designed DNA sequences. *Spectrochim Acta A* **2020**, *242*.

[31] Lin, P. H.; Chen, R. H.; Lee, C. H.; Chang, Y.; Chen, C. S.; Chen, W. Y. Studies of the binding mechanism between aptamers and thrombin by circular dichroism, surface plasmon resonance and isothermal titration calorimetry. *Colloid Surface B* **2011**, *88* (2), 552–558.

[32] Grueso, E.; López-Pérez, G.; Castellano, M.; Prado-Gotor, R. Thermodynamic and structural study of phenanthroline derivative ruthenium complex/DNA interactions: Probing partial intercalation and binding properties. *J Inorg Biochem* **2012**, *106* (1), 1–9.

[33] Mahadevan, S.; Palaniandavar, M. Spectroscopic and Voltammetric Studies on Copper Complexes of 2,9-Dimethyl-1,10-phenanthrolines Bound to Calf Thymus DNA. *Inorganic Chemistry* **1998**, *37* (4), 693–700.

[34] Sass, S.; Stöcklein, W. F.; Klevesath, A.; Hurpin, J.; Menger, M.; Hille, C. Binding affinity data of DNA aptamers for therapeutic anthracyclines from microscale thermophoresis and surface plasmon resonance spectroscopy. *Analyst* **2019**, *144* (20), 6064–6073.

[35] Cai, S.; Yan, J.; Xiong, H.; Liu, Y.; Peng, D.; Liu, Z. Investigations on the interface of nucleic acid aptamers and binding targets. *Analyst* **2018**, *143* (22), 5317–5338.

[36] Dam, D. H. M.; Lee, R. C.; Odom, T. W. Improved in vitro efficacy of gold nanoconstructs by increased loading of G-quadruplex aptamer. *Nano letters* **2014**, *14* (5), 2843–2848.

[37] Liu, Y.; Le, C.; Tyrrell, D. L.; Le, X. C.; Li, X.-F. Aptamer binding assay for the E antigen of hepatitis B using modified aptamers with G-quadruplex structures. *Anal Chem* **2020**, *92* (9), 6495–6501.

[38] Chen, J. A.; Jin, Y. T.; Ren, T. T.; Wang S.; Wang, X. H.; Zhang, F. Y.; Tang, Y. W. A novel terbium (III) and aptamer-based probe for label-free detection of three fluoroquinolones in honey and water samples. *Food Chem* **2022**, *386*, 132751.

[39] Serrano, M. J.; Mata, L.; Pellicer, S.; Segura-Gil, I.; Razquin, P.; Pagán, R. Development and validation of a rapid lateral flow test for the detection of fluoroquinolones in meat and blood. *Food Control*. **2024**, *156*, 110116.

[40] Yin, X. H.; Zhong, Y. J.; Chen, A. L.; Bao, T. Y.; Deng, Q. F.; Zhang, Y.; Yang, R. A triple-channel sensor array utilizing fluorescent carbon dots for simultaneous discrimination and detection of multiple fluoroquinolones. *Talanta*, **2024**, *279*, 126608.